

Efficient polyatomic interference reduction in plasma-source mass spectrometry *via* collision induced dissociation†

Glen P. Jackson,^a Fred L. King^b and Douglas C. Duckworth^{*a}

^aChemical Sciences Division, Oak Ridge National Laboratory, P. O. Box 2008, Oak Ridge, TN 37831-6375, USA. E-mail: duckworthdc@ornl.gov; Tel: (865) 576-6296

^bDepartment of Chemistry, West Virginia University, P. O. Box 6045, Morgantown, WV 26506-6045, USA

Received 18th March 2003, Accepted 30th June 2003

First published as an Advance Article on the web 22nd July 2003

Evidence is provided that illustrates quadrupole ion traps can be used to selectively attenuate strongly bound diatomic ions occurring at the same nominal mass as an analyte ion of interest. Dissociation rates for TaO⁺ ($D_0 \sim 750 \text{ kJ mol}^{-1}$) are found to be at least an order of magnitude larger than the loss rate of Au⁺ due to scattering under “slow heating” resonance excitation conditions at $q_z = 0.67$ and using neon as the bath gas. This rate difference is sufficient for the selective removal of this strongly-bound diatomic ion over the loss of the Au⁺ at the same mass-to-charge ratio. Other examples of quadrupole ion trap CID for the selective reduction of common plasma-generated species are also evaluated by examining the dissociation of GdO⁺ in the presence of Yb⁺, and Cu₂⁺ in the presence of Te⁺. In each case, a different method of applying the excitation signals is presented, and the attenuation rates for the diatomic species due to CID are substantially larger than scattering losses for the bare metal ions. Evidence is also presented that demonstrates CID can be accomplished in concert with a slow mass analysis scan, thereby providing a means of (1) eliminating polyatomic ions (formed in the plasma or reaction cell) over an extended mass range, (2) recovering metal ion signal from the metal-containing polyatomic ions, and (3) minimizing deleterious secondary reactions of product ions.

Introduction

Plasma ion sources for mass spectrometry, such as inductively coupled plasmas (ICP) and glow discharges (GD), are recognized as valuable tools for inorganic analyses.^{1,2} Yet, over two decades of development in ICP-MS and GD-MS have not fully addressed the detrimental effects of polyatomic spectral interferences. The ideal mass spectrometric approach to minimize or alleviate such effects would: (1) apply to all polyatomic interferences; (2) apply to atomic isobars; (3) eliminate or separate polyatomic ions with high selectivity relative to atomic ions; (4) remove polyatomic interferences completely; (5) maintain analyte sensitivity (*i.e.*, full retention of atomic ion signal without focusing, scattering, or chemical losses); and (6) would not otherwise compromise analytical performance. Although no ideal approach has been (or is expected to be) found, several approaches have been found that address many of these issues.³⁻⁶

The use of instrumentation capable of mass resolving interferences is the most straightforward and effective means of approaching the problem but usually comes at a significant cost. However, as high resolution magnetic sector instruments become more affordable, their use in resolving interferences to achieve analyses that were once intractable is becoming more widespread. Yet, there remain instances where the resolution necessary to achieve separation of analyte and interferent is unavailable or is precluded by the associated sacrifice of analyte ion signal intensity.³ Fourier transform ion cyclotron resonance mass spectrometers afford unsurpassed mass resolving power, but present many challenges for their application in quantitative elemental analysis.^{4,5}

Another approach, recently described in an excellent review by Tanner *et al.*,⁷ employs chemical resolution of interfering ions, wherein atomic and polyatomic ions undergo chemical reactions to differing degrees in pressurized reaction cells. Differences in chemical reactivity that afford resolution of atomic ion interferences may rely on (1) charge neutralization of interfering atomic and polyatomic ions or (2) selective adduct formation involving atomic or polyatomic ions. Chemical resolution proves to be highly effective for many reactions, particularly those involving discharge gas-related species. Though hydrogen, ammonia, and methane have been found to be versatile reactants for many interferences, a universal reagent is not likely to be identified given the diverse thermochemistry and kinetics that result in reactivities that range from unreactive to extremely reactive. Some reactions can result in detrimental secondary reactions and clustering. Secondary reactions are reduced through the use of selective band-pass filtering that results in instability and ejection of precursor ions of m/z values outside of the bandpass.⁶

Collision induced dissociation (CID) is another approach to polyatomic interference reduction. In the CID approach polyatomic (and atomic) ions undergo energetic collisions with a neutral target gas species. Upon collision, ion kinetic energy is converted into vibrational energy sufficient to dissociate the molecular ions. Although this approach has not received much attention recently, several groups in the late 1980s and early 1990s reported the use of double and triple quadrupole mass analyzers to achieve this reduction in interferences from glow discharge and inductively coupled plasmas.⁸⁻¹¹ Discharge gas-related atomic ions were reduced *via* charge transfer reactions, and CID afforded preferential loss of polyatomic over analyte atomic ions. Even very strongly bound species ($> 700 \text{ kJ mol}^{-1}$) were completely dissociated, but such results were often accompanied by unacceptable analyte losses. The best results showed atomic ion loss of

†Presented at the 2003 European Winter Conference on Plasma Spectrochemistry, Garmisch-Partenkirchen, Germany, January 12-17, 2003.

approximately 50% of the analyte intensity while polyatomics were reduced by two orders of magnitude.^{9–11}

Other investigations into the utility of CID for ICP-MS applications were not as promising. In an early report by Douglas, loss cross sections of atomic and polyatomic ions were measured, and the results indicated that negligible gains were anticipated due to charge transfer reactions between atomic ions and the target gases employed.⁸ This conclusion was substantiated soon thereafter by Rowan and Houk.⁹ Unlike organic applications, where 90% fragmentation is sufficient for structural identification, atomic mass spectrometry requires complete or quantifiable elimination of chemical interferences with minimal loss of atomic ions. CID for atomic mass spectrometry was largely abandoned, presumably due to conflicting reports regarding losses in analyte sensitivity.

The reason for conflicting results is not clear but may arise from differences in ion kinetic energies employed and how they affect collisional energy transfer and ion trajectories inside the collision cell. The maximum amount of energy that can be converted into internal excitation in a single collision is

$$E_{\max} = [M_t/(M_t + M_p)] \times E_{\text{lab}}$$

where M is the mass of the target (t) and parent ion (p).^{7,12} E_{lab} is the kinetic energy in the laboratory frame of reference. Two reports from the Marcus group showed that an $E_{\text{lab}} \leq 20$ eV resulted in a higher relative loss rate of copper diatomic (Cu_2^+) to copper atomic ions than was observed at an $E_{\text{lab}} = 40$ eV.^{11,13} The same observation is implicit in the work of Rowan and Houk⁹ where the best obtained CID discrimination occurred at low E_{lab} energies (0–5 eV). When cross sections for atomic and diatomic ions were measured at $E_{\text{lab}} = 50$ eV, similar loss cross sections were observed. Cross sections for lower energies were not reported.

By analogy with Beer's Law,

$$I/I_0 = e^{-n\sigma L}$$

the ratio of the transmitted ion intensity (I) from a linear quadrupole to the incident ion intensity (I_0) will decrease *via* CID exponentially with target number density (n), reaction pathlength (L), and loss cross section (σ). This cross section will include losses arising due to CID, ion–neutral reactions (including charge exchange), and scattering. In quadrupole ion traps, reaction time replaces the reaction pathlength. At low E_{lab} values scattering is minimized, but the degree of dissociation is too low for useful reduction of polyatomic populations in the time frame (pathlength) typically used in linear quadrupole collision cells. The latter is made worse by collisional cooling in the collision cell.¹⁴ This suggests that the optimal approach would utilize multiple low energy collisions over a longer time period (or pathlength) to vibrationally excite polyatomic ions and minimize atomic ion losses.

Quadrupole ion traps can be employed to effect such a slow heating process for polyatomic interferences. Ions can be stored for long periods (several 100 ms) and made to undergo continuous, selective acceleration at low kinetic energies (generally <5 eV) in a pressurized environment. A tutorial review article by McLuckey and Goeringer describes slow heating techniques in quadrupole ion traps.¹⁵ An important aspect of quadrupole ion trap collisional activation is that, in contrast to CID in linear quadrupole collision cells, only selected ions undergo acceleration in ion traps based on m/z specific resonance excitation frequencies. As a result, other analytes are not accelerated and needlessly scattered. Quadrupole ion traps allow both chemical resolution^{16–18} and CID⁵ to be employed for the elimination of common spectral interferences.

Optimal conditions for CID of strongly bound diatomic ions have been reported that allow full retention of parent ions and

complete recovery of product metal ions (*i.e.*, no scattering losses).¹⁹ Dissociation kinetics for this CID process have been measured and utilized for the determination of bond energies.²⁰ Additionally, the kinetics involved in CID of diatomic ions have been modeled, showing that it is consistent with a multiple collision (slow heating) process.²¹ Simulations suggest that internal temperatures obtained in the dissociation of TaO^+ ($D_0 \sim 750$ kJ mol⁻¹) exceed ten thousand degrees, consistent with the observation that even the most tenacious interferences can be eliminated through CID in the quadrupole ion trap. With the ion trap approach, collision energies lower than those associated with linear quadrupoles are sufficient to successfully fragment many metal polyatomic ions. As a result of the step-wise introduction of energy into vibrational excitation, the difference in ionization potentials of the isobaric atom and the collision gas should not be exceeded by any single collision, thereby precluding any losses associated with charge exchange.²²

The purpose of this study is to provide evidence for the highly selective dissociation of a strongly-bound metal monoxide ion interference without significant scattering losses of an atomic ion at the same nominal m/z under conditions optimized for CID of the diatomic interference. The isobaric pair studied, $^{181}\text{Ta}^{16}\text{O}^+$ and $^{197}\text{Au}^+$ (m/z 197), serves as an interesting model because the tantalum oxide ion forms a very strong bond (~ 750 kJ mol⁻¹)²³ and represents the difficult extreme in which a diatomic interference ion would require dissociation in the presence of an analyte ion. Additionally, two more examples of isobaric interference are presented to demonstrate the general utility and selectivity of this CID approach. In these cases isotope ratios are used to verify the low scattering rates of the atomic ion species. Evidence is also provided that the diatomic ion interferences can actually be attenuated during the data acquisition scan function of the quadrupole ion trap, *viz.*, the isobars can be removed as the mass spectrum is collected. Future applications of this approach should hold promise for removing interferences across the entire mass spectral range and addressing undesirable secondary chemical reactions that may occur during the ion trapping period.

Experimental

A pulsed dc glow discharge was used as the ion source in a design similar to that described previously.²⁴ A 0.5 Torr Ne glow discharge ion source was interfaced to a commercial quadrupole ion trap mass spectrometer (Teledyne Discovery 3DQ, formerly Mountainview, CA) modified for the injection of externally generated ions. Ions were focused *via* a three-lens electrode configuration and injected through a grounded endcap electrode of the three electrode quadrupole ion trap configuration. The ion trap electronics provided the trigger used to signal a pulse generator (BNC 8010, Berkley Nulceonics Corp., San Rafael, CA), the square-wave output of which was amplified by a high voltage power supply (Model OPS3500, Kepco, Flushing, NY, USA) that sustained the -1.5 kV pulsed glow discharge. This mode of operation was effectively a continuous discharge, which was turned off during ion manipulation and detection.

A typical scan function involved a 2–50 ms injection period, with a single frequency excitation signal applied to resonantly eject the matrix ions and a radiofrequency trapping potential cutoff (high pass filter) to prevent low mass ion storage. A 50–100 ms reaction period followed during which metal ions were allowed to react with molecular oxygen at $q_z = 0.2$. A 5 ms ion isolation period using mass selective instability²⁵ and filtered noise fields (FNF)²⁶ was then used to obtain the m/z ions of interest. Following a 10 ms ion cooling period at $q_z = 0.2$, the resonance excitation signal was applied in a dipolar fashion at

$q_z \sim 0.67$.²⁷ Product ions were allowed to cool (10 ms at $q_z = 0.2$) before mass analysis. Mass analysis was then performed using axial modulation and ions ejected through one endcap were detected *via* a Channeltron electron multiplier (Model 4773G, Galileo Electro-optics, Sturbridge, MA, USA). Variations on these scan functions are presented later. In all cases, resonance excitation was applied in a dipolar fashion between the endcaps and without phase-locking to the ion trapping potential on the quadrupole ion trap ring electrode (thus precluding high mass resolution measurements).

To generate tantalum oxide ions in the presence of gold ions, tantalum metal powder was first pressed into a gold pin (which served as the cathode material). Neon, purified using in-line getters (Model GC50, SAES Pure Gas, Inc., San Luis Obispo, CA, USA), was used as the discharge gas at 1 Torr and as the quadrupole ion trap bath gas at 0.5 mTorr (corrected). Ion manipulation using FNF frequencies²⁶ was used to obtain either TaO^+ or a mixture of TaO^+ and Au^+ at mass 197, as follows. To obtain TaO^+ at mass 197 in the absence of ^{197}Au , all the ions of mass 181 (Ta^+) and 197 (TaO^+ and Au^+) were collected during the ion injection period. The ions at m/z 197 were then resonantly ejected at a $q_z = 0.67$ with an excitation voltage ~ 500 mV_{pp} at 226 kHz. The Ta^+ ions were then allowed to form TaO^+ by reacting them with molecular oxygen admitted to the trapping region *via* a manual leak valve at a pressure of $\sim 1 \times 10^{-6}$ Torr. The unreacted Ta^+ ions remaining after 80 ms were resonantly ejected leaving TaO^+ ions as the only surviving species at m/z 197. If the same procedure is followed, with the exception of the first isolation step, one obtains (within 5%) the same number of TaO^+ ions at mass 197 with the addition of (a) the TaO^+ ions formed in the glow discharge and trapped during the ion injection period and (b) the Au^+ ions.

To measure the CID rate, as described previously,¹⁹ resonance excitation at 226 kHz frequency was applied at a $q_z = 0.67$. A second, larger, FNF voltage was simultaneously applied to the Ta^+ product ions, ejecting them and preventing the forward reaction occurring. Mass spectra could be obtained following various excitation times in order to determine the dissociation rate of TaO^+ . The same approach was repeated, with and without the resonance ejection of Ta^+ , in the presence of Au^+ to determine the effect of the excitation voltage on the scattering rate of Au^+ .

To dissociate GdO^+ in the presence of Yb^+ , a small amount of isotopically enriched ($\sim 50:50$ $^{154}\text{Gd}:^{155}\text{Gd}$) Gd_2O_3 was pressed on to a Yb metal pin. Dual GD pulses were used in each quadrupole ion trap scan function in order to obtain the desired ratios of GdO^+ to Yb^+ . In the first pulse, FNF waveforms were used to selectively trap the bare Gd^+ ions. The second pulse was used to add the desired amount of Yb^+ and subsequent reactions of Gd^+ with added oxygen ($\sim 1.6 \times 10^{-6}$ Torr) formed the required interferences. The Yb^+ ion abundance remains virtually unchanged during this time because its reaction with O_2 is endothermic, and the reaction is very slow.²⁸ Ions between m/z 165–180 were then isolated and kinetically cooled at a $q_z \approx 0.3$ for 20 ms. The method of dissociation in this case involved a fixed frequency excitation voltage of 370 mV_{pp} at 226 kHz and various rf drive amplitudes. In this way, ions of different m/z are sequentially brought into resonance with the excitation voltage and the degree of dissociation/scattering can be evaluated for each m/z .

To dissociate copper dimers in the presence of tellurium a small quantity of tellurium oxide was pressed onto the surface of a copper pin. At high glow discharge voltages (~ 1500 V at ~ 1 Torr) Cu_2^+ and Te^+ could be generated in appropriate ratios for this study. After isolating and cooling Cu_2^+ and Te^+ ions, broadband FNF frequency excitation (60 mV_{pp}) was applied over the m/z range 120–140, so as to cause all the ions to undergo excitation at the same time. Because the copper ions are so much lighter than the dimer ions, the low mass cut-off

value, and hence the trapping potential and well depth for the dimers, had to be lowered to ensure that the bare copper ions were recaptured after dissociation.

Results and discussion

The use of collision induced dissociation in quadrupole ion traps is an appealing approach to the reduction of polyatomic interferences because it is in principle applicable to all interferences. Historically, the limitation of the CID approach has been the inadequate degree of selectivity in the reduction of polyatomic relative to atomic analyte ions. The slow-heating approach to CID in quadrupole ion traps has been shown to be effective for the dissociation of diatomic ions, but never in the presence of an analyte atomic ion of interest. Three same-mass element-molecular interferent pairs— TaO^+/Au^+ (m/z 197), GdO^+/Yb^+ (m/z 170–171), and $\text{Cu}_2^+/\text{Te}^+$ (m/z 126–128)—were investigated to determine relative dissociation rates and to demonstrate the general utility of the approach. Several modes of ion trap operation used in this investigation are reported, including a novel scanning approach for multiple isotope (element) CID.

$^{181}\text{Ta}^{16}\text{O}^+$ in the presence of $^{197}\text{Au}^+$. Tantalum oxide interference in the presence of gold atomic ions was chosen as the initial case study for this investigation. Tantalum oxide forms a particularly strong bond, ~ 750 kJ mol⁻¹,²³ and it is therefore difficult to quantitatively dissociate using linear quadrupole systems.¹⁰ Values of the integrated mass spectral peak area measured for different resonance excitation times were used to study the effects of resonance excitation on the dissociation and scattering rates of TaO^+ and Au^+ , respectively.

It should be noted that a constant O_2 concentration (1 μTorr) was intentionally added to the trapping region by necessity to form the oxides used in illustrating CID as a means of reducing interferences. Ta^+ reacts rapidly to form TaO_2^+ *via* the intermediate TaO^+ .¹⁹ Under resonance excitation, TaO^+ forms no measurable quantities of TaO_2^+ . If oxide ions are formed in the plasma source, and O_2 and H_2O are absent from the trap, then the forward oxidation reactions will not compete with the dissociation reactions due to the low partial pressure of O_2 . Because O_2 is added in these experiments, it is necessary to prevent the oxidation reaction of the Ta^+ dissociation product as described below.

Fig. 1A shows the ion signals obtained when TaO^+ is dissociated at 320 mV_{pp} in the absence of Au^+ . In this example the Ta^+ product ions are trapped during the dissociation event. The total ion current profile shows a 98% recovery for a 1 ms excitation period. This recovery decreases to 85% for a 50 ms excitation and represents a 4 s⁻¹ loss rate due to scattering or ion molecule reactions of the parent ions during the extended resonance excitation period. More efficient recovery is possible at lower excitation amplitudes, with a corresponding decrease in dissociation rate.

After 20 ms, steady-state signals are obtained between the CID reaction rate and the forward oxidation reaction rate. Altering the amplitude of the excitation frequency can shift the relative intensities of the 'equilibrium' signals. Higher excitation voltages increase the dissociation rate and promote the abundance of Ta^+ over TaO^+ (this will be discussed in Fig. 2), yet the oxidation reaction still prevents an accurate measurement of the dissociation rate. Fig. 1B shows that when a mass specific, simultaneous ejection voltage is applied to the Ta^+ product ion, it can be efficiently ejected from the trap, allowing parent ion loss rates to be measured. In the absence of scattering and ion-molecule reactions, this loss rate is the CID rate. A plot of $-\ln([\text{TaO}^+]_t/[\text{TaO}^+]_{t=0})$ versus time gives a linear plot¹⁹ with a phenomenological dissociation rate of

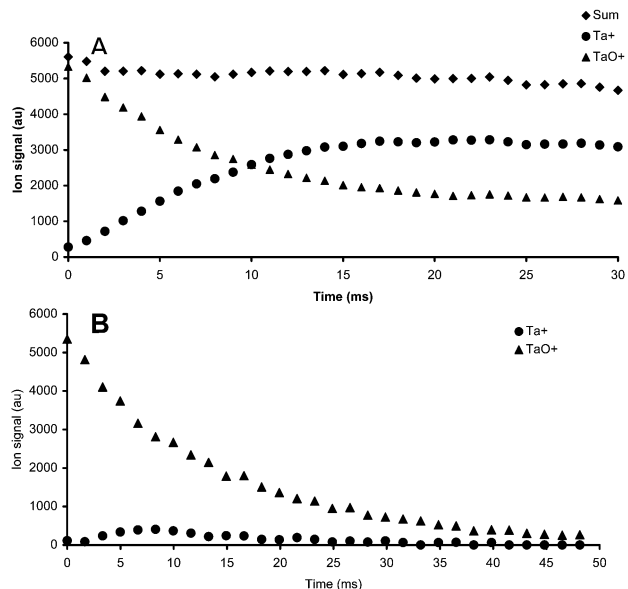


Fig. 1 A, Ion signals obtained at 320 mV_{pp} excitation amplitude, Ta⁺ not ejected and B, ion signals obtained at 250 mV_{pp} with resonance ejection on Ta⁺.

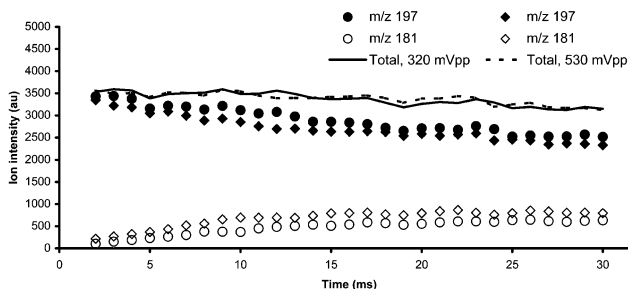


Fig. 2 Plot of ion signal versus excitation time showing the effect of excitation amplitude on the steady-state signals of Ta⁺ at *m/z* 181 and TaO⁺ and Au⁺ at *m/z* 197.

68 s⁻¹ at 250 mV_{pp}, where [TaO⁺]_t is the ion signal at time *t* and [TaO⁺]_{t=0} is the ion signal at time zero. Thus, the CID rate for TaO⁺ is 17 times greater than the total ion loss rate (4 s⁻¹) in the absence of Au⁺ in the ion trap.

Fig. 2 shows various ion signals measured as a function of the resonance excitation time obtained when TaO⁺ is dissociated in the presence of Au⁺. Ta⁺ is not simultaneously ejected during the dissociation event in these cases. The Au⁺ signal makes up approximately 60% of the signal at *m/z* 197. When a higher excitation voltage of 530 mV_{pp} is applied, the steady-state concentration of Ta⁺ increases compared with the value at 320 mV_{pp}. This is due to the increased dissociation rate at higher excitation amplitudes, balanced with the constant forward oxidation rate. At both voltages the total ion current decreases by ~5% over the 30 ms dissociation period, indicating a small degree of scattering. Because the Ta⁺ signal intensity reaches a steady-state value at approximately 20 ms, and does not measurably decrease thereafter, the ion losses are assigned to the scattering of Au⁺ ions. By attributing the losses in total ion signal to the loss of Au⁺, an upper limit of 5 s⁻¹ is calculated for the scattering rate of Au⁺. Rather surprisingly, the calculated scattering loss does not appear to be greatly affected by the excitation amplitude, indicating that the losses are consistent with ion trapping losses in the absence of resonance excitation.

To prevent TaO⁺ from continually forming through the oxidation of Ta⁺, the experiment was repeated with a resonance ejection of Ta⁺ during the dissociation step. The

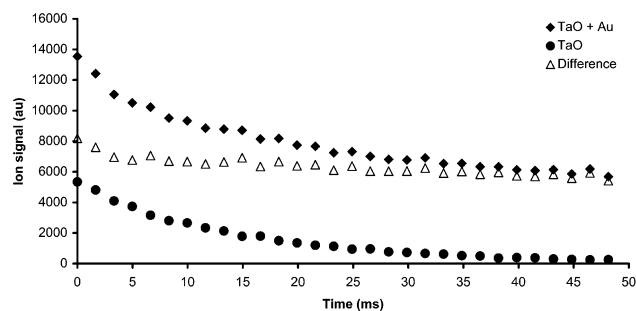


Fig. 3 Plot of the ion signal versus time showing the attenuation rate at *m/z* 197 with and without the presence of Au⁺.

experiment was performed first with only TaO⁺ ions present and then with TaO⁺ and Au⁺ present. The number density of TaO⁺ ions in each experiment was held constant. The ion signal at *m/z* 197 is plotted as a function of time in Fig. 3 with and without the presence of Au⁺. It is clear that the rate of ion loss at *m/z* 197 is very similar in each case. A plot of the difference between the two ion signals yields a steady-state value. With the evidence provided in Fig. 2—that the TaO⁺ readily dissociates and that the scattering loss of Au⁺ is <5 s⁻¹—the difference between the two slopes in Fig. 3 can be attributed to the signal due to Au⁺. The ‘steady-state’ signal also decreases at a rate of ~5 s⁻¹ and is comparable to the scattering rate of Au⁺ obtained earlier. The attenuation rate for Au⁺ ions is therefore at least an order of magnitude smaller than the attenuation rate of the isobaric TaO⁺ ions (68 s⁻¹). The attenuation rates would be expected to differ by a larger proportion in cases where the dissociation energy is less than that of TaO⁺, *i.e.*, for most diatomic interferences.

¹⁵⁴Gd¹⁶O⁺ and ¹⁵⁵Gd¹⁶O⁺ in the presence of ¹⁷⁰Yb⁺ and ¹⁷¹Yb⁺. Further evidence for the sustained trapping of atomic ions at conditions necessary for dissociating diatomic ions at the same mass can be gained by using elements with interferences at multiple isotopes. Fig. 4A shows a mass spectrum of the isotopes of Yb⁺ with interfering GdO⁺ present. GdO⁺ ions have a high dissociation energy of approximately 735 kJ mol⁻¹,²⁹ and again represent a particularly stubborn molecular interference. Histogram lines underneath the peaks show the natural isotopic composition for Yb⁺ and demonstrate that the ion signals at *m/z* 170 and 171 are significantly larger than expected for pure Yb.

Figs. 4B and 4C are examples of two CID mass spectra obtained as a fixed frequency (226 kHz) excitation potential (400 mV_{pp}) is applied in a dipolar fashion between the endcap electrodes. As the amplitude of the rf trapping potential applied to the ring electrode is increased in steps corresponding to 0.05 u increments, ions come into resonance with the 226 kHz excitation potential. In Fig. 4B, the excitation frequency is on-resonance with *m/z* 170. The ¹⁵⁴GdO⁺ ions are quantitatively dissociated, while the bare ¹⁷⁰Yb⁺ ions are retained. The same effect is seen in Fig. 4C when the excitation voltage comes into resonance with *m/z* 171.

This experiment provides evidence that it is possible to bring multiple ions into resonance with the resonance excitation potential to provide attenuation of multiple isobaric interferences. This method is of benefit in that each *m/z* species is swept through resonance and that resonance excitation occurs when the excited ions are held at the largest potential well depth. This allows larger excitation amplitudes to be applied, allowing the dissociation of strongly-bound diatomic ions while ensuring that the bare metal ions are held strongly in the center of the trap. It should be noted that resonance excitation amplitude tuning is critical for strongly bound diatomic ions. This is largely due to the high excitation voltage required to dissociate such strong bonds. In such situations, it is imperative to tune

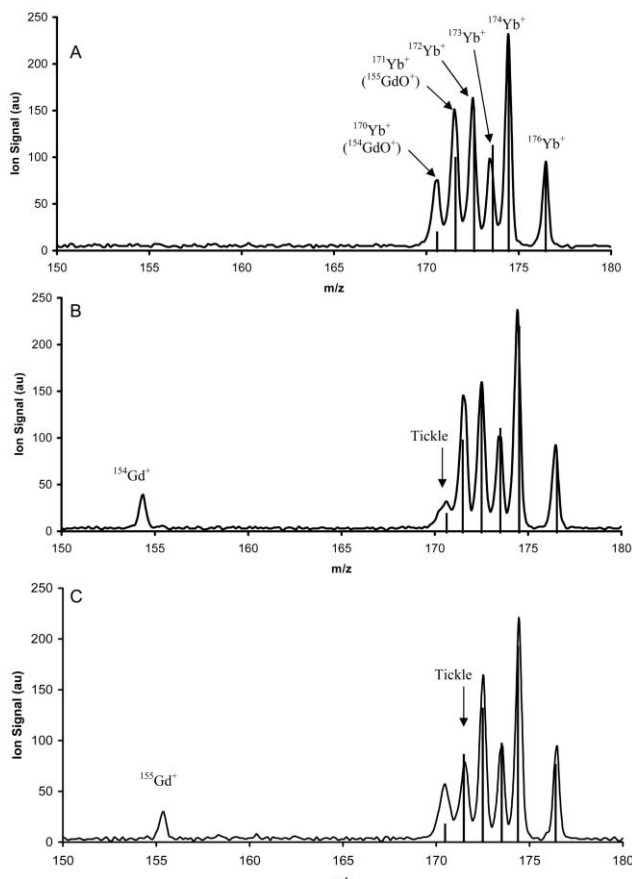


Fig. 4 A, Isotopes of Yb^+ with GdO^+ interfering at m/z 170 and 171, B, single frequency excitation on m/z 170, and C, single frequency excitation on m/z 171. Excitation amplitude of $370 \text{ mV}_{\text{pp}}$ at 226 kHz for 20 ms in 0.5 mTorr Ne .

the amplitude of the excitation potential while precisely on resonance.

$^{63,63}\text{Cu}_2^+$, $^{63,65}\text{Cu}_2^+$, and $^{65,65}\text{Cu}_2^+$ in the presence of $^{126}\text{Te}^+$, $^{128}\text{Te}^+$, and $^{130}\text{Te}^+$. Instead of sweeping all the masses through a single frequency excitation signal, one can also use broadband excitation to dissociate interferences over a wide mass range. An example of the broadband approach is given in Fig. 5 for the dissociation of copper dimers in the presence of tellurium atoms. Fig. 5a shows the mass spectrum of Te ions in the presence of copper dimer interferences. Isotopic analysis of the peaks was made and compared with the natural isotopic abundance of tellurium in Table 1. Before CID of molecular interferences, the apparent isotope ratios are particularly inaccurate, especially for the major isotopes at m/z 126, 128 and 130.

Fig. 5b shows the mass spectra acquired after a 20 ms broadband excitation ($60 \text{ mV}_{\text{pp}}$ at each m/z at $q_z \approx 0.3$). The dissociation of Cu_2^+ at this low trapping potential (low q_z) is made possible by the ease at which the dimer dissociates—its dissociation energy has been estimated³⁰ at $\sim 170 \text{ kJ mol}^{-1}$. In these studies, weakly bound interferences such as Cu_2^+ were considerably easier to dissociate than the extreme case of TaO^+ . The two isotopes of copper at m/z 63 and 65 are retained in the trap and display a reasonably accurate isotopic ratio (see Table 1). The uninterfered minor isotopes of Te are not scattered, even though they are exposed to the same excitation amplitude as the interfered isotopes. This is clearly evident in Table 1, where the isotopic distribution for the tellurium ions is now much closer to the expected distribution. (The isotopic ratios for tellurium in the complete absence of Cu_2^+ have not been measured using this ion trap, so mass biases have not been accounted for.) Not only can the atomic tellurium ions be

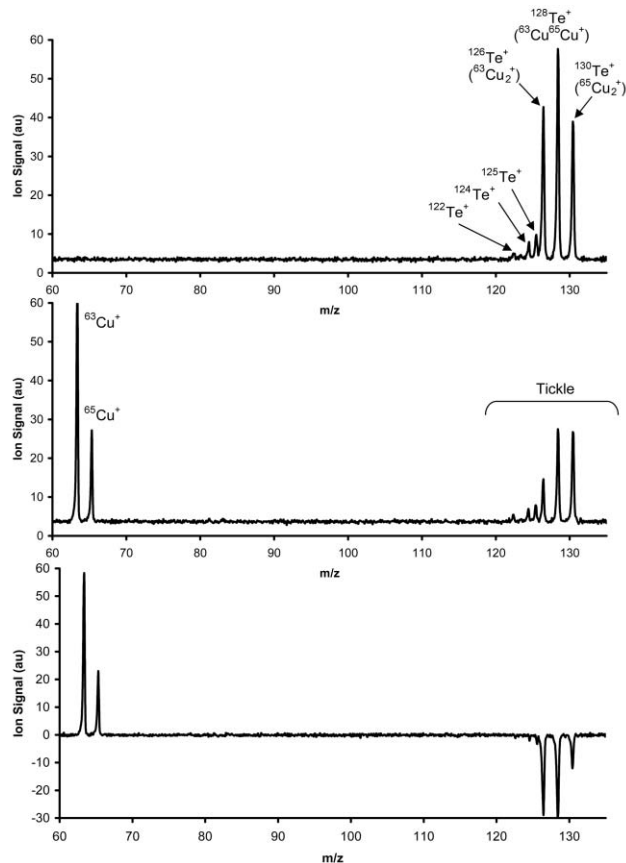


Fig. 5 A, Isotopes of Te^+ with Cu_2^+ interfering at m/z 126, 128 and 130; B, mass spectrum obtained after 20 ms , $60 \text{ mV}_{\text{pp}}$ multiple frequency excitation over the range m/z 120–140; and C, the difference taken between Figures A and B to show the quantitative recapture of dissociated Cu ions.

Table 1 Compares the relative isotopic abundance for some Te ions before and after the application of broadband excitation to remove interfering Cu_2^+ ions

m/z (identity)	Relative abundances ^a (%)		Natural isotopic abundance ³¹ (%)
	Before CID	After CID	
63 (Cu^+)	—	72.7	69.2
65 (Cu^+)	—	27.3	30.8
122 (Te^+)	1.9	2.8	2.6
124 (Te^+)	4.2	6.2	4.9
125 (Te^+)	6.0	7.1	7.1
126 (Te, Cu_2^+)	26.6	16.6	19.0
128 (Te, Cu_2^+)	36.1	33.0	31.7
130 (Te, Cu_2^+)	25.1	34.4	33.8

^aCalculated from peak areas.

separated from the interfering dimers of copper, but also the fragmentation products of the CID process—the bare copper ions—are retained for isotopic analysis.

Fig. 5c is the difference between Figs. 5a and 5b and demonstrates that if this procedure was carried out in a multi-element standard over a wide mass range it would be possible to determine the precursors to certain fragment ions. In this example, it is clear that the isotopic distribution of the copper dimer ions between m/z 126–130 produces the isotopic distribution observed at m/z 63 and 65 (Table 1). Although the sum of the peak heights at m/z 63 and 65 in Fig. 5c appears to be larger than the sum of the dimer ion peaks, integration of the peak areas reveals that charge is indeed conserved, *i.e.*, copper atomic ions do not spontaneously appear. The lower mass peaks are simply narrower.

One of the limitations in using the broadband excitation approach at a fixed q_z value is that ions of low m/z are trapped at smaller well depths. This restricts the ability to trap light ions during CID and thus the kinetic energy that can be imparted to the molecular ions. An alternative approach for achieving CID is to apply an excitation signal during the mass analysis scan in a manner allowing dissociation prior to resonance ejection. This is analogous to the axial modulation technique for mass range extension.²⁵ Axial modulation employs a supplemental frequency for resonance *ejection* prior to reaching the instability boundary ($q_z = 0.91$). In the application to CID, a supplemental resonance *excitation* frequency is used to effect CID during the scan. Bare metal product ions are retained at a higher q_z (<0.91) just before detection. Product ions fall at a high q_z and are stored for only a short time prior to detection (~ 6 ms at a scan rate of 3000 u s^{-1}). This has the added benefit of minimizing secondary reactions.

To test this approach, copper dimers formed in the glow discharge were isolated in the trap prior to CID excitation. A mass selective instability scan (rf amplitude ramp) was performed with a 451 kHz (336 mV) axial modulation frequency. A second fixed excitation frequency (110 kHz, 344 mV) was simultaneously applied in a dipolar fashion to the endcap electrodes. As the rf drive amplitude was increased to eject sequentially the lowest mass ions for detection, heavier ions sequentially came into resonance with the supplementary frequency. During on-resonance excitation, diatomics were dissociated whereas the product atomic species were retained at a higher q_z (due to a lower mass) than the parent ion. This approach is demonstrated in Fig. 6. The very small hump at m/z 47 reveals the time at which the dimer at m/z 126 first comes in to resonance with the dissociation voltage. The peak shows the dimer ions that are slightly scattered during the time they are being heated. The ramp rate used in this experiment was 3000 u s^{-1} (normal ramp rates are $\sim 12\,000 \text{ u s}^{-1}$) and this was close to the slowest possible ramp rate allowed by the software. This gives each copper dimer isotope approximately 0.3 ms of on-resonance excitation. Clearly, to obtain a greater degree of dissociation and less scattering, a slower acquisition speed and smaller voltage is required so that each isotope remains on-resonance for a longer time. However, because our current software restricts the scan speed, slower scan rates were not investigated.

By using a slower drive-amplitude ramp rate it should be possible to dissociate more completely isobaric interferences during the acquisition ramp of the ion trap. As higher masses come into resonance with the excitation frequency it might also be necessary to simultaneously ramp the amplitude of the excitation frequency. This is because in ion trap CID experiments heavier ions require larger excitation voltages than lighter ions to yield the same dissociation rate, even when the dissociation energies are the same.²⁰ This latter

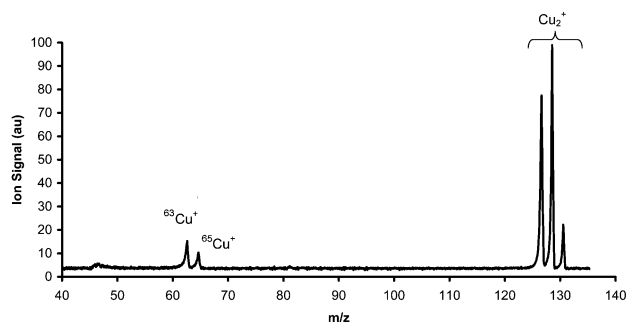


Fig. 6 Mass spectrum obtained when Cu_2^+ is subjected to resonance excitation at 110 kHz during the acquisition period of the scan function. Each isotope of the dimer ion is on-resonance for approximately 0.3 ms.

technique—increasing the excitation amplitude to dissociate higher mass interferences during the slowed acquisition scan—might provide the most appealing approach to multiple element determinations as it utilizes a constant and optimal q_z value for all m/z ions and minimizes the possibility of unwanted reactions of atomic ions with residual or contaminant gases. This is because atomic ions are scanned out of the trap and detected with minimal time for subsequent reactions.

Conclusions

Collision induced dissociation in quadrupole ion traps has now been demonstrated—albeit in select, yet challenging examples—to address the first five characteristics of the ideal approach for eliminating interferences in atomic mass spectrometry (as posed in the introduction). CID in the trap appears to be a universal method that is highly selective in the reduction of polyatomic over atomic ions. This approach has been applied to both weakly and strongly bound diatomic interferences with negligible losses of same-mass atomic ions. Both chemical resolution and CID are possible in quadrupole ion traps and serve as complementary approaches, with the former allowing atomic isobars to be separated. Remaining challenges exist in the routine implementation of these techniques and the further demonstration of the analytical characteristics. Further work is planned in which certified standards are available to validate the claims of the usefulness of this technique for elemental analysis.

Acknowledgements

Research sponsored by the Division of Chemical Sciences, Geosciences, and Biosciences, Office of Basic Energy Sciences, U.S. Department of Energy, under contract DE-AC05-00OR22725 with Oak Ridge National Laboratory, managed and operated by UT-Battelle, LLC. FLK and GPJ gratefully acknowledge support from the U.S. Department of Energy, DE-FG02-00ER45837.

References

- 1 C. M. Barshick, *Inorganic Mass Spectrometry*, eds. C. M. Barshick, D. C. Duckworth and D. H. Smith, Marcel Dekker, Inc., New York, 2000.
- 2 J. W. Olesik, *Inorganic Mass Spectrometry*, eds. C. M. Barshick, D. C. Duckworth and D. H. Smith, Marcel Dekker, Inc., New York, 2000.
- 3 L. Moens, F. Vanhaecke, J. Riondato and R. Dams, *J. Anal. At. Spectrom.*, 1995, **10**, 569.
- 4 D. C. Duckworth and C. M. Barshick, *Anal. Chem.*, 1998, **70**, 709A.
- 5 D. C. Duckworth, J. R. Eyler and C. H. Watson, *Inorganic Mass Spectrometry*, eds. C. M. Barshick, D. C. Duckworth and D. H. Smith, Marcel Dekker, Inc., New York, 2000.
- 6 S. D. Tanner and V. I. Baranov, *J. Am. Soc. Mass Spectrom.*, 1999, **10**, 1083.
- 7 S. D. Tanner, V. I. Baranov and D. R. Bandura, *Spectrochim. Acta, Part B*, 2002, **57**, 1361.
- 8 D. J. Douglas, *Can. J. Spectrosc.*, 1989, **34**, 38.
- 9 J. T. Rowan and R. S. Houk, *Appl. Spectrosc.*, 1989, **43**, 976.
- 10 F. L. King and W. W. Harrison, *Int. J. Mass Spectrom. Ion. Processes*, 1989, **89**, 171.
- 11 D. C. Duckworth and R. K. Marcus, *Appl. Spectrosc.*, 1990, **44**, 649.
- 12 S. A. McLuckey, *J. Am. Soc. Mass Spectrom.*, 1991, **3**, 599.
- 13 Y. Mei, D. C. Duckworth, P. R. Cable and R. K. Marcus, *J. Am. Soc. Mass Spectrom.*, 1994, **5**, 845.
- 14 D. J. Douglas and J. B. French, *J. Am. Soc. Mass Spectrom.*, 1982, **3**, 398.
- 15 S. A. McLuckey and D. E. Goeringer, *J. Mass Spectrom.*, 1997, **32**, 461.
- 16 S. A. McLuckey, G. L. Glish, D. C. Duckworth and R. K. Marcus, *Anal. Chem.*, 1992, **64**, 1606.
- 17 G. C. Eiden, C. J. Barinaga and D. W. Koppelaar, *J. Anal. At. Spectrom.*, 1996, **11**, 317.

- 18 G. C. Eiden, C. J. Barinaga and D. W. Koppenaal, *Rapid Commun. Mass Spectrom.*, 1997, **11**, 37.
- 19 D. C. Duckworth, D. E. Goeringer and S. A. McLuckey, *J. Am. Soc. Mass Spectrom.*, 2000, **11**, 1072.
- 20 G. P. Jackson, F. L. King, D. E. Goeringer and D. C. Duckworth, *Int. J. Mass Spectrom.*, 2002, **216**, 85.
- 21 D. E. Goeringer, D. C. Duckworth and S. A. McLuckey, *J. Phys. Chem. A*, 2001, **105**, 1882.
- 22 K. L. Busch, G. L. Glish and S. A. McLuckey, *Mass Spectrometry/ Mass Spectrometry: Techniques and Applications of Tandem Mass Spectrometry*, VCH Publishers, New York, 1988.
- 23 Calculated using the equation $\text{BDE}(\text{TaO}^+) = \text{BDE}(\text{TaO}) + \text{IE}(\text{Ta}) - \text{IE}(\text{TaO})$. Value for $\text{BDE}(\text{TaO}) = 799 \text{ kJ mol}^{-1}$ is taken from *CRC Handbook of Chemistry and Physics*, ed. D. R. Lide, CRC Press, New York, 81st edn., 2000. ; values for $\text{IE}(\text{Ta}) = 714 \text{ kJ mol}^{-1}$ and $\text{IE}(\text{TaO}) = 764 \text{ kJ mol}^{-1}$ are taken from S. G. Lias, J. E. Bartmess, J. F. Liebman, J. L. Holmes, P. D. Levin and W. G. Millard, *J. Phys. Chem. Ref. Data*, **17**, 1988, suppl. 1.
- 24 D. C. Duckworth, D. H. Smith and S. A. McLuckey, *J. Anal. At. Spectrom.*, 1997, **12**, 43.
- 25 G. C. Stafford, P. E. Kelly, J. E. P. Syka, W. E. Reynolds and J. F. J. Todd, *Int. J. Mass Spectrom. Ion Processes*, 1984, **60**, 85.
- 26 D. E. Goeringer, K. G. Asano, S. A. McLuckey, D. Hoekman and S. W. Stiller, *Anal. Chem.*, 1994, **66**, 313.
- 27 J. N. Louris, R. G. Cooks, J. E. P. Syka, P. E. Kelly, J. G. C. Stafford and J. F. J. Todd, *Anal. Chem.*, 1987, **59**, 1677.
- 28 G. K. Koyanagi and D. K. Bohme, *J. Phys. Chem. A*, 2001, **105**, 8964.
- 29 M. S. Chandrasekharaiah and K. A. Gingerich, *Handbook on the Physics and Chemistry of the Rare Earths*, ed. J. K. A. Gschneidner and L. Eyring, Elsevier, New York, 1989.
- 30 A. A. Radzig and B. M. Smirnov, *Reference Data on Atoms, Molecules and Ions*, Springer, Berlin, 1985, ch. 11.
- 31 *CRC Handbook of Chemistry and Physics*, ed. D. R. Lide, CRC Press, New York, 2000.